Chemical Physics 140 (1990) 429–438
North-Holland

INFRARED SPECTROSCOPIC AND PHOTOCHEMICAL STUDY OF WATER–OZONE COMPLEXES IN SOLID ARGON

L. SCHRIVER [1], C. BARREAU [2] and A. SCHRIVER [3]

Laboratoire de Spectrochimie Moléculaire (CNRS, UA 508), Université Pierre et Marie Curie, 4 Place Jussieu, 75252 Paris Cedex 05, France

Received 27 June 1989

Infrared spectroscopy has been coupled with the matrix isolation technique, firstly for a study of the molecular complexes between ozone and water, secondly to investigate the mechanism of the water photooxidation by ozone at 15 K by UV light. The 1 1, 1 2 and 2.1 complexes are isolated and mainly characterized by a shift in the infrared absorption of the H_2O (D_2O) submolecule. Force field calculations involving anharmonicity corrections allows us to conclude into the non-equivalence of the two OH oscillators within the 1.1 complex. This result suggests the formation of a very weak hydrogen bond of the type HOH...OO_2. By photolysis of the water–ozone mixture in solid argon ($\lambda < 310$ nm), formation of H_2O_2 with very small amounts of O_2H and OH is observed. This process occurs through the reaction between the $O(^1D)$ atom generated by photodissociation of O_3 belonging to the one $H_2O{:}O_3$ pair and the water molecule of the same pair, without diffusion of the oxygen atom.

1. Introduction

The fragmentation of O_3 by light of visible and UV wavelengths plays a vital role in stratospheric chemistry. Atomic oxygen produced either in $O(^3P)$ or $O(^1D)$ states ($\lambda < 310$ nm) allows oxidation of atmospheric compounds. In particular oxidation of the source gas SO_2 and its subsequent reaction with water to form sulphuric acid is of interest. In this way, complex formation can have significant effects on reaction rates. In our attempt to study the photochemical process involving H_2O–SO_2–O_3 we have been led to examine in detail the infrared spectra of $(H_2O)_m(SO_2)_n$ complexes trapped in solid argon [1]. The present study is undertaken to isolate and characterize complexes between H_2O and O_3 by the matrix isolation technique. No structural determination of the species has been published up to now. Only a few data have been reported by Nord [2] in a short paper upon some complexes involving O_3 isolated in solid nitrogen, and by Suenram et al. [3] in a brief communication upon the microwave spectrum of the ozone–water complex. In addition, we have also investigated the photooxidation of H_2O, the atomic oxygen being produced in situ by the photolysis of matrix isolated ozone and water at various wavelengths. It is known that the metastable $O(^1D)$ atom reacts with atmospheric water molecules yielding two OH radicals. Detailed information on this exothermic reaction in the gas phase has been reported by Gericke and Comes [4]. Results are presented in two parts; the first part is devoted to the identification and structure of the $(H_2O)_m(O_3)_n$ complexes; the second part points out the photooxidation of H_2O by O_3.

2. Experimental

Ozone was generated by Tesla coil discharge of oxygen (normal isotopic, Air Liquide N45 purity) in a pyrex tube immersed in liquid N_2; residual O_2 was removed by pumping at 77 K. Water and D_2O (CEA 99% stated isotopic purity) were used after "freeze–pump–thaw" purification in a vacuum line. Argon (Air Liquide N50 purity) was used without further

[1] Also at Université Paris Nord, France.
[2] Also at Laboratoire de Chimie Physique Marine, CNRS UA 353.
[3] Also at Laboratoire de Physique Moléculaire et Atmosphérique, UPR 136

purification. The gas mixtures containing Ar as the matrix gas are made in a 1 ℓ bulb by standard manometric techniques and sprayed through a one inlet system onto the cold CsI window maintained at 19 K. The deposition rate was ≈10 mmol/h. Two cryogenic refrigerator systems have been used: (i) a liquid helium cryostat (TBT) for short irradiation time, (ii) a closed-cycle helium refrigerator (Air Products displex model 202 A) for long irradiation time. Photolysis was carried out at ≈11 K using (i) a high-pressure mercury lamp (Philips 93110, 90 W), (ii) a xenon lamp (Schoeffel 150 W), (iii) a low-pressure mercury arc home built.

Additionally, cutoff filters such as Schott WG 280 (cutoff 270 nm) and Schott WG 345 (cutoff 320 nm) were used for photolysis and a 10 cm H_2O cell to eliminate infrared irradiation. The spectra were recorded on a Perkin–Elmer model 580 IR spectrometer. The resolution varied depending on the spectral region: 1.8 cm^{-1} at 3700 cm^{-1} and 0.9–0.6 cm^{-1} in the range 1600–400 cm^{-1}.

3. Identification and structure of the $(H_2O)_m(O_3)_n$ complexes

3.1. Results

Experiments with H_2O, D_2O, HDO and O_3 will be described. The spectrum of water in solid argon has been studied in great detail by Ayers and Pullin [5] and Bentwood et al. [6], and the spectrum of ozone has been reported by Andrews and Spiker [7]. In the following only new bands induced in the matrix will be discussed. Two kinds of experiments were carried out, a first set with low concentration in water (typically H_2O/Ar: 1/1000) and a second with high water content (H_2O/Ar 1/200). In both cases, the ozone concentration was varied from 1/200 to 1/100.

3.1.1. Spectra at high dilution in water

3.1.1.1. H_2O fundamentals. Addition of water traces to O_3/Ar mixtures (H_2O/O_3/Ar=0.5/5/1000) leads to the appearance of one new band in the domain of each fundamental mode as shown in figs. 1 and 2: 3726.5, 3632.5 and 1592.5 cm^{-1}. These bands which keep a constant intensity ratio (respectively 1/0.18/0.95) are assigned to the H_2O O_3 1:1 complex. The observed frequencies are close to the ones measured for the water molecule acting as electron donor in $(H_2O)_2$ trapped in argon. Nevertheless their identification is trivial because for such concentrations the water dimer is nearly non-existent, and the intensity of the new bands is abnormally strong.

When the ozone concentration was increased, two new weak bands emerged in the ν_1 and ν_2 region at 3603 and 1597 cm^{-1} respectively. In the ν_3 region the identification of a new band at 3704 cm^{-1} requires careful intensity measurements because of closeness of this band to that of a water dimer line. But the intensity ratio of the two ν_3 and ν_1 acceptor stretching bands (I_{3707}/I_{3574}) in H_2O/Ar binary mixtures has been found equal to 0.40 against 2 in H_2O/O_3/Ar matrices. Thus these three new lines are assigned to a $1 \cdot 2$ H_2O/O_3 complex.

3.1.1 2. D_2O fundamentals Three new bands, not observed in the spectra of D_2O/Ar binary mixtures, were measured in D_2O/O_3/Ar matrices at 2765.5, 2654 and 1176.5 cm^{-1} (fig. 3). The last one is in full overlap with a ν_2 dimer line but is still present at low D_2O content. All these bands have the same concentration dependence and are assigned to the 1:1 complex. The isotopic ratios of 1.348, 1.369 and 1.354 for ν_3, ν_1, ν_2 respectively are in good agreement with usual values found for other weak complexes involving water.

Bands assignable to the 1:2 $D_2O(O_3)_2$ complex are difficult to identify because of their weakness and of their near coincidence with dimer lines. Careful comparison between the D_2O band intensities in binary and ternary matrices allows identification of three new lines at 2745 (ν_3), 2635.5 (ν_1) and 1179 cm^{-1} (ν_2).

3.1.1.3. HOD fundamentals The simultaneous presence of hydrogen and deuterium in the water samples leads to the appearance of one additional band in each of the ν_{OH}, ν_{OD} and δ_{HOD} spectral regions: 3691, 2697, 1399 cm^{-1}. These bands are assigned to the three fundamentals of HDO in the HDO:O_3 complex.

When the ozone concentration was increased three new weak bands at 3671, 2681 and 1403 cm^{-1} in partial overlap with HOD dimer bands were identified and tentatively assigned to the $1 \cdot 2$ HOD/O_3 complex.

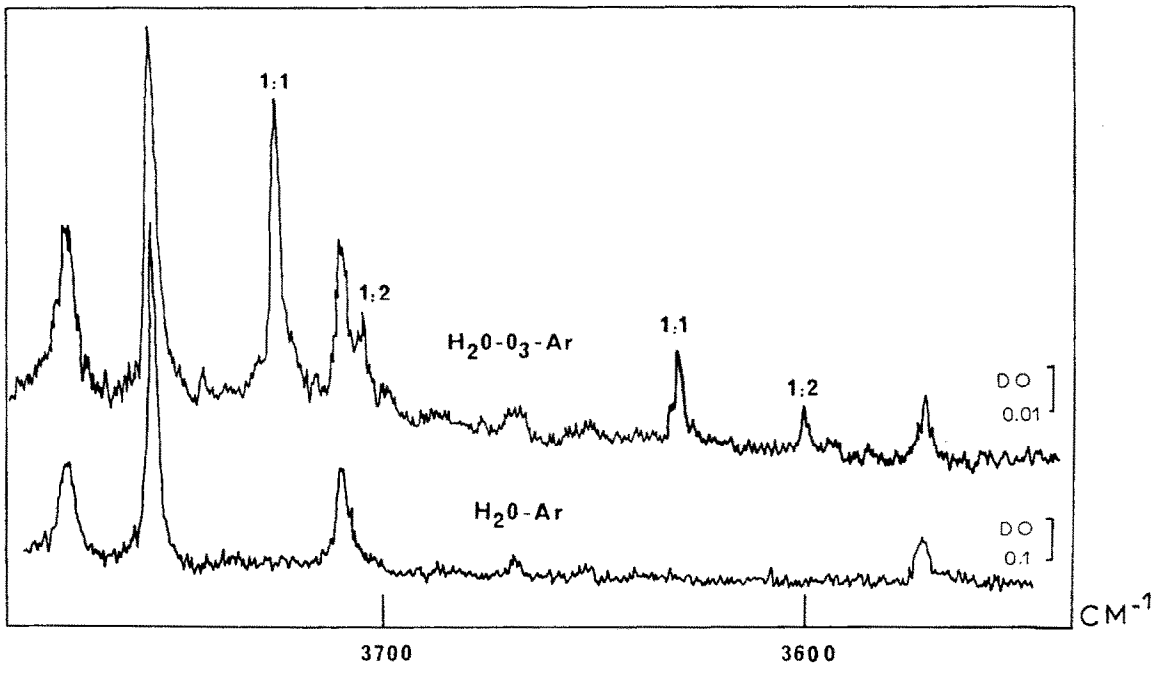

Fig. 1. Water complex absorptions with O_3 in argon matrix at 10 K in the range 3800–3500 cm^{-1} ($H_2O/O_3/Ar$: 0.5/5/1000); spectrum of a H_2O/Ar matrix without O_3 is included for comparison.

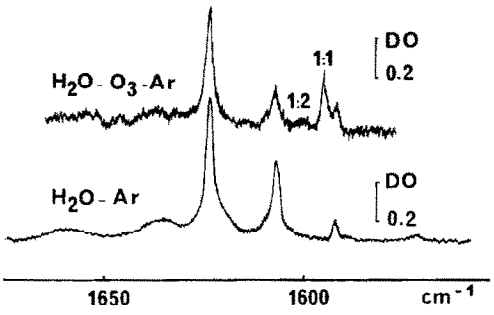

Fig. 2. Water complex absorptions with O_3 in argon matrix at 10 K in the range 1700–1550 cm^{-1} ($H_2O/O_3/Ar$:0.5/5/1000); spectrum of H_2O/Ar matrix without O_3 is included for comparison.

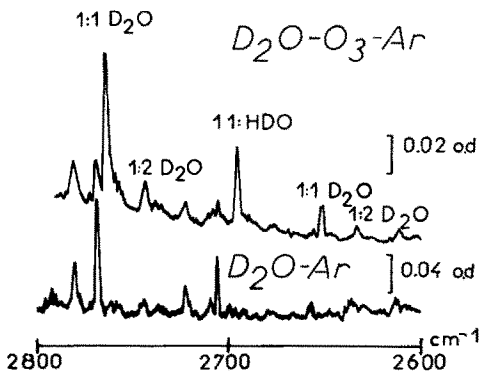

Fig. 3. OD stretching bands of the $D_2O:O_3$ complex at 11 K ($D_2O/O_3/Ar$: 1/5/500). Lower panel D_2O/Ar = 1/500.

3.1.1.4. Ozone absorption regions. The presence of water induces new weak satellites in the ozone spectral regions. They are respectively measured at 1107, 708 and 1046 cm^{-1} above ν_1, ν_2, ν_3 of ozone as shown in fig. 4. A new band at 2114.5 cm^{-1} was also resolved from its respectively precursor combination $\nu_1 + \nu_3$. Sample annealing produced a weak growth in these bands without other signals. Table 1 gathers the frequencies and assignments for the 1:1 and 1:2 complexes.

3.1.2. Spectra at high concentration in water

Several spectra at $H_2O/O_3/Ar \approx 1/1/250$ were recorded using natural or deuterium enriched water

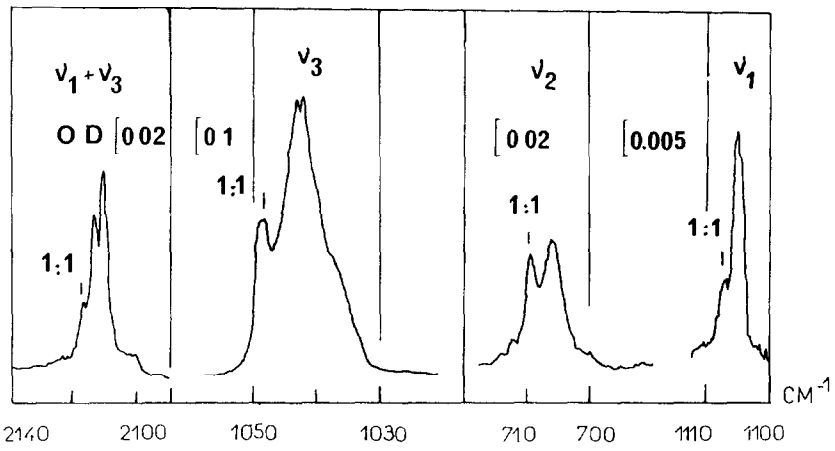

Fig. 4 Ozone complex absorptions in argon matrix at 10 K (H_2O/O_3/Ar 1/10/1000).

Table 1
Observed frequencies (cm^{-1}) and proposed assignments for H_2O/O_3, D_2O/O_3 and HDO/O_3 complexes in argon matrices

H_2O	D_2O	HDO	Assignment
3726.5	2765 5	3691	ν_3 (1 1)
3704	2745	3671	ν_3 (1 2)
3632.5	2654	2697	ν_1 (1 1)
3603	2635 5	2681	ν_1 (1 2)
1597	1179	1403	ν_2 (1 2)
1592 5	1176 5	1399	ν_2 (1 1)

samples. The high complexity of the water spectra due to the presence of many polymeric bands makes the identification of the complexes difficult and requires special care. Subtraction of spectra in the presence and in the absence of O_3 allows identification of new bands distinct of the bands previously assigned to the 1:1 and 1·2 species and characteristic of at least one *m* 1 complex. Unfortunately no complementary information was obtained from the examination of the O_3 spectral regions.

3.1.2.1. H_2O fundamental region. Two well isolated bands at 3620 and 3559 cm^{-1} are unambiguously identified as being due to H_2O/O_3 complexes. In addition two other absorptions at 3720 and 3544 cm^{-1} which appear as shoulders to monomeric and polymeric water bands could be assignable to some *m*.1 complex. In the ν_2 region a new line at 1601 cm^{-1} is also observed.

3.1 2.2. D_2O, HOD fundamental region. In the OD stretching region three new bands are readily identified at 2645, 2607 and 2604 cm^{-1}. In addition two other features at 2759 and 2696 cm^{-1} in overlap with the monomer lines of D_2O and HOD and another line at 2742 cm^{-1} appearing as a shoulder to the dimer HOD signal are also assignable to aggregates with ozone containing several water molecules. In the OH region, a new band at 3686.5 cm^{-1} in overlap with one HOD line arises from the same species. This assignment is based on the observation that the relative intensity of this band is stronger in the presence than in the absence of ozone. In the bending region one band at 1394.5 cm^{-1} which appears as a shoulder to a dimer absorption can be tentatively assigned to a 2:1 species.

3.2 Discussion

Structure and bonding of the 1:1 and 1:2 water–ozone species will be considered from their observed infrared absorptions.

3.2 1. 1:1 complex

The 1:1 complex is unambiguously characterized by the three fundamentals of complexed water. The small shifts are rather close to those measured for the proton acceptor molecule in the water dimer. A comparable situation has been previously observed for the complex between SO_2 (isoelectronic of O_3 in the va-

lence shell) and H_2O in argon and interpreted in terms of charge transfer complex with an O...S interaction in which H_2O plays the role of electron donor and SO_2 that of a Lewis acid [1]. In such a complex the water molecule retains C_{2v} symmetry and the two equivalent OH oscillators couple as efficiently as in free water. This type of structure seems unlikely here in regard of the decoupling scheme displayed in fig. 5. This scheme shows that the coupling of the two OH and OD oscillators is not symmetrical leading to the conclusion that the two oscillators are not equivalent. In order to verify this assumption we have performed on water a force field calculation using the method described in ref. [1]. A good fit has been obtained between calculated and observed frequencies with the hypothesis of the non-equivalence of the two OH oscillators (table 2). These results confirm that the complexation proceeds through hydrogen bonding rather than through charge transfer as in the $H_2O:SO_2$ case. The recent, not yet published studies in the gas phase by microwave spectroscopy point out the same conclusion about the structure [3]. In the case of the $HDO:O_3$ species, the presence of only one band in the OD region, typical of a hydrogen bonded oscillator, shows the existence of only one isotopomer HOD...O_3; the formation of D bond rather than H bond has already been observed for other complexes [1,8,9] and interpreted in term of zero-point energy difference between the two forms. Comparison between the water spectral shifts in the $H_2O:O_3$ complex and those in other complexes where water acts as a proton donor, shows that the $H_2O:O_3$ complex is remarkably weak, e.g. weaker than those with unsaturated hydrocarbon molecules [9]. If we consider the often assumed approximately linear relationship between the enthalpy of complexation ΔH_f and the frequency shift of ν_1(HDO) for a series of proton acceptor molecules [10], one may expect a ΔH_f value for the water–ozone complex less than 1 kcal mol^{-1}. This weak interaction explains that the $\nu_1/\nu_2/\nu_3$ intensity ratios in the complex (0.18/0.95/1) are rather close to those of monomer water (0.15/1/1.05) in N_2 matrix [11], suggesting a weak charge transfer upon complexation [12]. Spectral shifts of the ozone submolecule are also observed upon complexation; they noticeably differ from those observed in the $HF:O_3$ complex [13]. The three modes are blue shifted by about 5 cm^{-1} without noticeable change in their relative intensity while in the $HF.O_3$ complex, the ν_3 mode was red shifted 13 cm^{-1}, the ν_1 and the ν_2 mode were blue shifted by 12 and 10 cm^{-1} re-

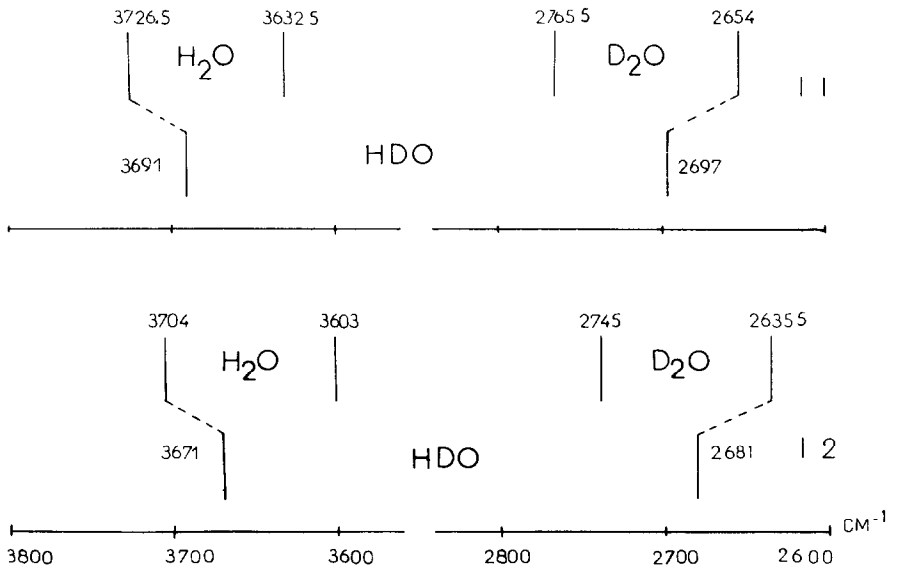

Fig. 5. Coupling scheme of the OH and OD oscillators of the water molecule engaged in 1 1 and 1:2 complexes with O_3.

Table 2
Comparison between observed and calculated frequencies (cm^{-1}) of the water moiety in the water–ozone complex (1 1 complex) trapped in argon, with the following assumed bond: $O_2O...H-O-H$ [a]

	H_2O		D_2O		HOD	
	obs.	calc.	obs.	calc	obs.	calc.
ν_1	3632.5	3630.1	2654	2654 2	2697	2700
ν_2	1592 5	1592 3	1176.5	1174 9	1399	1400.8
ν_3	3726.5	3726 2	2765.5	2766 0	3691	3691 3

[a] Force constants (mdyn $Å^{-1}$) $F_{r1}=7.61$, $F_{r2}=7.517$, $F_{rr}=-0.0678$, $F_{r1\delta/R}=0.18$, $F_{\delta/R^2}=0.707$ For HOD complex $F_{OH}=F_{r1}$ and $F_{OD}=F_{r2}$ (hydrogen bonding) Anharmonicity coefficients [1] are as follows D_2O: for ν_1 1 0136, for ν_2 1.0093, for ν_3 1 0136 HOD: for ν_1 1 0136, for ν_2 1 0041, for ν_3 1

spectively with a relative intensity increasing of the ν_1 mode.

3.2 2 1.2 complex

In the presence of a large excess of O_3 with respect to H_2O, the 1:2 species is responsible of three new bands in the OH stretching and bending regions. Their frequencies are slightly red shifted from the values for the 1·1 species (21, 29 and 5 cm^{-1} respectively for ν_3, ν_1, ν_2). The 1:2 complex is expected to occur from the 1:1 complex by the addition of a second O_3 molecule. Starting from the structure of the 1 1 complex discussed above, two possibilities remain available for bonding, either through the formation of a second weak OH...O bond or through an O...O charge transfer interaction. In the first case the two complexed OH are equivalent and the OH/D coupling effect between the two OH (OD) oscillators is symmetrical. In the second case the additional O_3 molecule which interacts with the water oxygen atom gives an asymmetrical structure. The observed isotopic dilution results (fig. 5) show that as in the case of the 1 1 complex, the coupling is asymmetrical which leads to the conclusion that the two OH oscillators are not equivalent. This result is confirmed by force field calculations performed on the water moiety (table 3).

Table 3
Comparison between observed and calculated frequencies (cm^{-1}) of the water moiety in the water–$(O_3)_2$ complex (1 2 complex) with following assumed bonds:

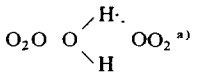

	H_2O		D_2O		HOD	
	obs.	calc	obs.	calc.	obs	calc
ν_1	3603	3605.3	2635 5	2636 8	2681	2679.6
ν_2	1597	1595.0	1179	1176.9	1403	1402.2
ν_3	3704	3701.6	2745	2746.9	3671	3670.7

[a] Force constants (mdyn $Å^{-1}$). $F_{r1}=7\ 5275$, $F_{r2}=7\ 3925$, $F_{rr}=-0.0585$, $F_{r1\delta/R}=0.28$, $F_{r2\delta/R}=0.10$, $F_{\delta/R^2}=0\ 71$

4. Photolysis of the H_2O–O_3–Ar matrix. Results and discussion

4 1 Identification of the reaction products

Irradiation experiments performed on $O_3/H_2O/Ar \approx 6/1/600$ matrices using the full light of the xenon lamp destroyed O_3 and led to the appearance of two main new features, one at 3588 cm^{-1} and the two others at 1275 and 1270 cm^{-1} (fig. 6). These bands are respectively assigned to the ν_1, ν_2, ν_6 modes of the hydrogen peroxide molecule on the basis of the infrared spectrum of H_2O_2 in solid argon reported by Lannon et al. [14]. Use of D_2O instead of H_2O leads to the frequency shifts expected for D_2O_2 (bands at 2646.5, 982 and 952 cm^{-1} associated with ν_1, ν_2 and ν_6 respectively). With long irradiation time, two new weak bands at 3452 and 3414 cm^{-1} are observed showing formation of very small amounts of OH [15,16] and O_2H radicals [17]. Note that the photodestruction of solid ozone in excess ice at 308 mm leads also to the H_2O_2 product [18].

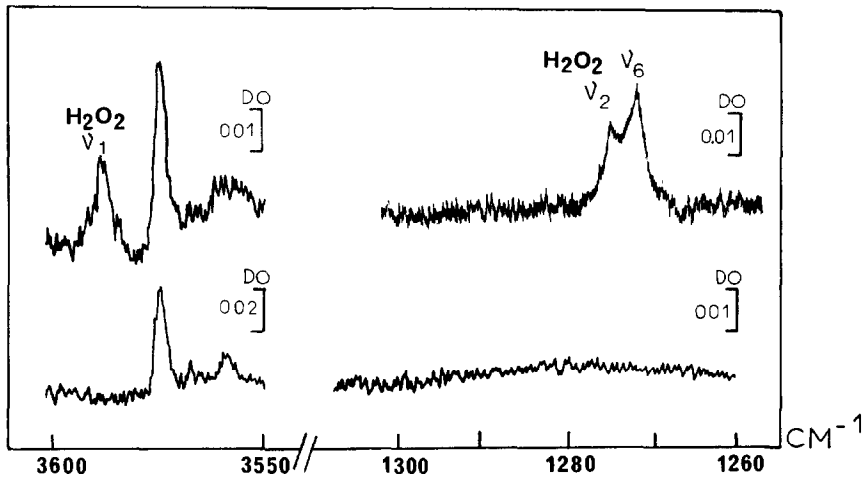

Fig. 6. Growth of absorptions in an Ar matrix at 12 K. $H_2O/O_3/Ar = 1/6/600$ after full irradiation of the xenon lamp during 1 h.

4 2. Domain of efficient radiation

Other experiments were carried out with various lamps and filters, as reported in section 2, in order to check the frequency range of the radiation efficient for reaction.

The formation of H_2O_2 was only observed at wavelength lower than 320 nm. If one takes into account the values of the quantum yield for the formation of $O(^3P)$ and $O(^1D)$ atoms as a function of the irradiation wavelength [19] one is led to conclude that the irradiation domain efficient for production of H_2O_2 corresponds mainly to the formation of $O(^1D)$ atoms. Note also that the destruction of O_3 was only observed for irradiation at $\lambda < 320$ nm which suggests that there is a nearly 100% cage recombination of the $O(^3P)$ with O_2. This observation is in good agreement with a previous study on VUV photolysis of CO_2 in various matrices where migration of the O atom in the ^3P state did not happen in argon at low temperature [20].

4.3. Time evolution of the bands

One or two of the following reactions can occur:

$$H_2O + O(^1D) \rightarrow H_2O_2 , \quad (1)$$

$$H_2O{:}O_3 + h\nu \rightarrow H_2O_2 + O_2 . \quad (2)$$

Reaction (1) involves the intensity decrease of the free water bands while in reaction (2) only the intensity decrease of the bands of the 1·1 complex is expected. Fig. 7 displays the time evolution of some bands of H_2O, O_3 and H_2O_2, as recorded in a typical irradiation study during 3 h. Two characteristics deserve attention. Firstly, as expected the H_2O_2 bands bands grow in intensity with irradiation time while the O_3 band intensity decreases. Secondly, in the ν_3(OH) water region, a significant change is the decrease in intensity of the $O_3{:}H_2O$ complex band at 3726 cm^{-1} while none of the free water absorptions have been observed to change in intensity. Thus there is strong evidence that the growth of H_2O_2 is due to reaction (2) within the $H_2O{:}O_3$ 1·1 complex. This assumption is confirmed by experimental results illustrated in fig. 8. This figure shows the integrated intensity of the 1276 cm^{-1} band of H_2O_2 as a function of the irradiation time, 24 h corresponding to the total disappearance of the ozone. An important observation is that the H_2O_2 absorption band intensity approaches a limit $A^{\infty}_{H_2O_2}$ after 11 h irradiation; the behaviour expected in a first-order reaction is limited by the initial reactive $H_2O{:}O_3$ pairs while O_3 is not yet totally consumed.

4.4. Rate equation

In the assumption of a first-order process, the quantitative expression for the rate of the reaction can

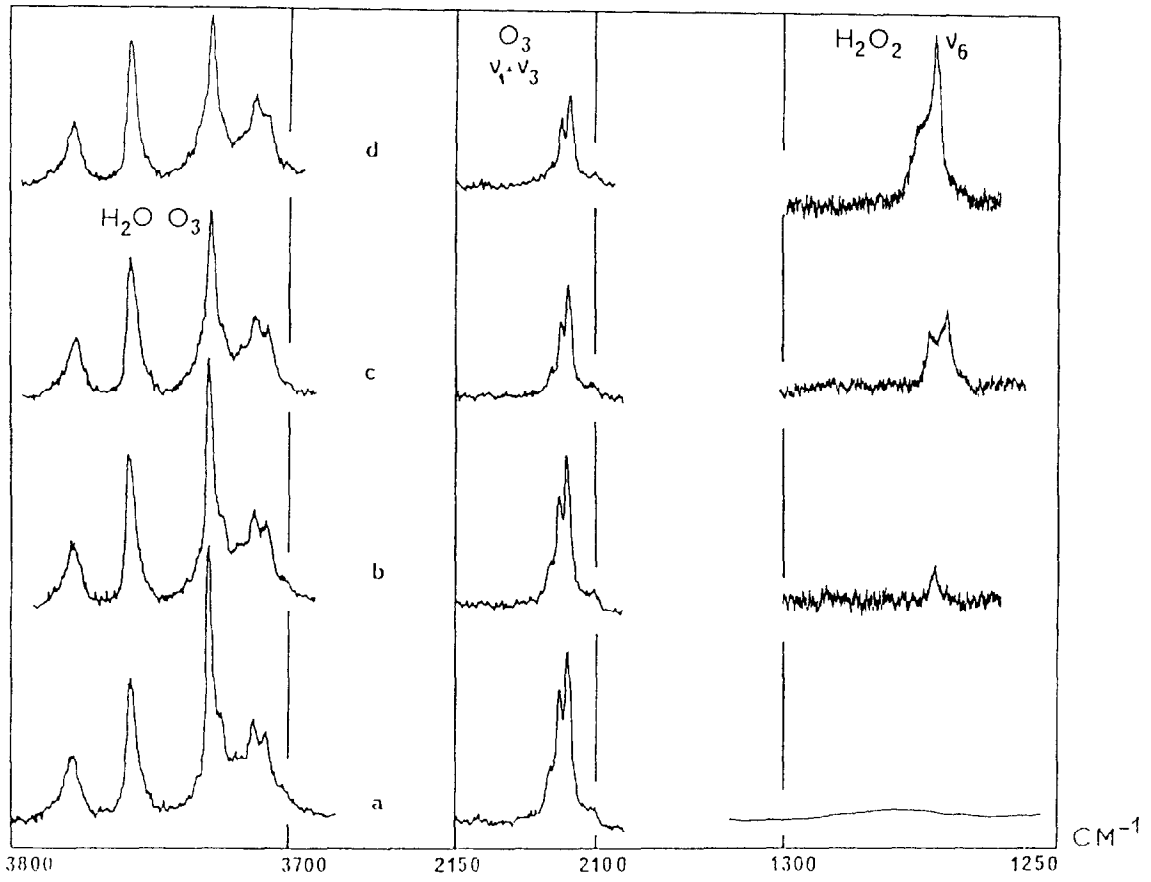

Fig. 7 Evolution of the spectrum of a H_2O/O_3/Ar (1/6/600) matrix with the time of irradiation (high-pressure mercury lamp with pass band filter WG 280) Irradiation time: (a) 0, (b) 30, (c) 40, (d) 150 min)

be obtained from the schematic process·

$$H_2O \cdot O_3 \xrightarrow{h\nu} H_2O_2 + O_2 .$$

Integrating the first-order rate equation from time 0 to t we obtain

$$[C]_t = [C]_0 e^{-kt},$$

in which $[C] = [H_2O\ O_3]$ and subscript 0 refers to the initial time.

Since one H_2O_2 is produced from one complex

$$[H_2O_2]_t = [C]_0(1 - e^{-kt})$$

Expressed in terms of either $H_2O{:}O_3$ integrated intensity A_C or H_2O_2 integrated intensity $A_{H_2O_2}$, these equations become:

$$A_C^t = A_C^0\, e^{-kt}$$

and

$$A_{H_2O_2}^t = A_{H_2O_2}^{\infty}(1 - e^{-kt}) .$$

A_C^0 and $A_{H_2O_2}^{\infty}$ can be experimentally measured and thus k can be determined by curves fitting the measurements of the product intensity versus time for each product (C or H_2O_2) without knowledge of extinction coefficient. Plots of $\ln(A_t^C/A_0^C)$ or $\ln[(A_{H_2O_2}^{\infty} - A_{H_2O_2}^t)/A_{H_2O_2}^{\infty}]$ versus time for a typical experiment with a high-pressure mercury lamp and the WG 280 filter are shown in fig. 9 The resulting straight line and excellent agreement between the two kinds of measurements give evidence for a first-order process. The first-order rate constant deduced for the

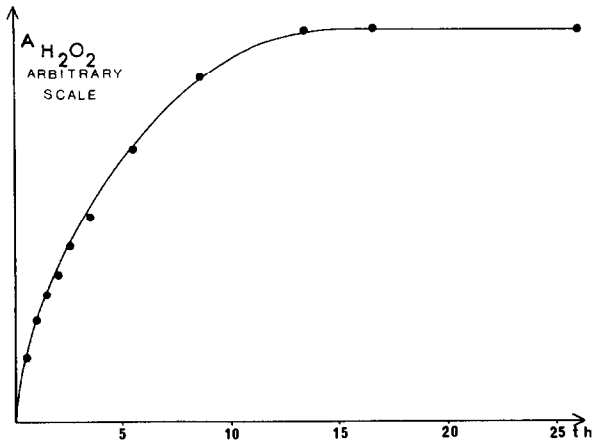

Fig. 8 Integrated intensity of the H_2O ν_6 absorption versus irradiation time (high-pressure mercury lamp with pass band filter WG 280).

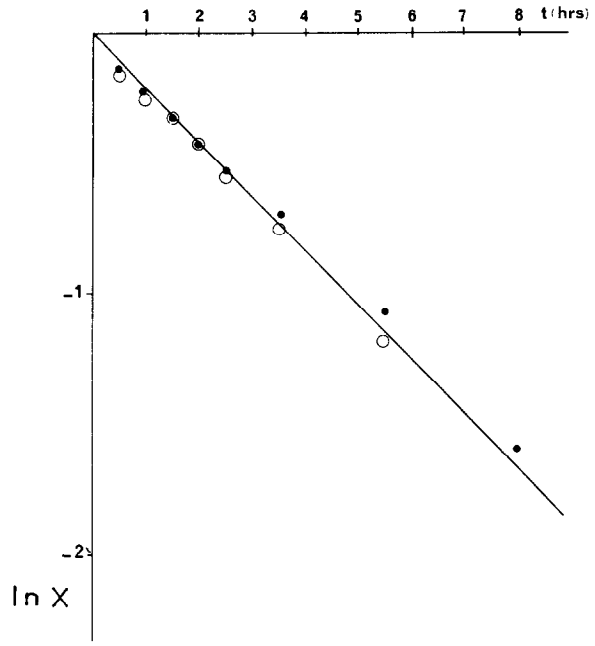

Fig. 9 Plots of ln X versus time spent by the sample (H_2O/O_3/Ar: 1/6/600) in the radiation of the high-pressure mercury lamp with pass band filter WG 280 (○) refers to $X=A_C/A_C^0$. (●) refers to $X=A^{\infty}_{H_2O_2}-A_{H_2O_2}/A^{\infty}_{H_2O_2}$.

production of H_2O_2 is 0.20 ± 0.05 h^{-1} at 12 K under the experimental irradiation conditions.

4.5. Mechanism

Two mechanisms for the formation of H_2O_2 are possible: either an insertion process:

$$H_2O{:}O_3 \xrightarrow{h\nu} [H_2O{\cdot}O(^1D)+O_2]^* \rightarrow HOOH+O_2\,, \quad (3)$$

or a dissociation/recombination process:

$$H_2O{:}O_3 \xrightarrow{h\nu} [H_2O{\cdot}O(D_1)+O_2]^* \rightarrow 2OH+O_2\,, \quad (4)$$

$$OH+OH \rightarrow HOOH\,. \quad (5)$$

Reaction (4) has been evidenced in the gas phase [4], and in matrix, recombination (5) could be expected to occur since the two hydroxyl radicals are trapped in the same site. In this assumption, the low yield of OH might be due to some escape. However, we suggest that the insertion process (3) is more probable on the basis of similar observations in low-temperature matrices [21,22] which allow the stabilization of primary products of photolysis. In gas phase, the H_2O_2 primary product could be not observed, H_2O_2 breaking down to OH+OH.

Acknowledgement

The authors are very grateful to Professor J.P. Perchard for fruitful discussions. They thank Mrs. D. Carrere for technical assistance.

References

[1] A Schriver, L. Schriver and J P. Perchard, J. Mol. Spectry. 127 (1988) 125.
[2] L. Nord, J. Mol. Struct. 96 (1982) 37.
[3] R.D. Suenram, F.J. Lovas, J. Gillies and C W Gillies, Communication to 43th Molecular Spectroscopy Symposium, Columbus OH, June 1988.
[4] K.H. Gericke and F.J. Comes, Chem. Phys. 65 (1982) 113
[5] G.P. Ayers and A.D.E. Pullin, Spectrochim. Acta 32 A (1976) 391.

[6] R.M. Bentwood, A.J. Barnes and W.J. Orville-Thomas, J Mol Spectry 84 (1980) 391.
[7] L Andrews and R C. Spiker Jr., J Phys Chem 76 (1972) 3208
[8] S.A Clough, Y Beers, G.P. Klein and L.S. Rojhman, J Chem Phys. 59 (1973) 2254.
[9] A Engdahl and B Nelander, Chem Phys. Letters 113 (1985) 49
[10] A Engdahl and B Nelander, Chem Phys. 100 (1985) 273
[11] L Schriver, A. Burneau and J P Perchard, J. Chim Phys (Paris) 82 (1985) 9.
[12] B A. Zilles and W.B. Person, J Chem. Phys. 79 (1983) 65.
[13] L Andrews, R Withnall and R.D. Hunt, J Phys. Chem. 92 (1988) 78.
[14] J.A. Lannon, F.D. Verderame and R.W. Anderson Jr., J Chem Phys. 54 (1971) 2212.
[15] N. Acquista, L.T Schoen and D R. Lide Jr , J. Chem Phys 48 (1968) 1534
[16] B.M Cheng, Y P. Lee and J.F. Ogilvie, Chem. Phys. Letters 151 (1988) 109.
[17] M E. Jacox and D E Milligan, J. Mol. Spectry. 42 (1972) 495.
[18] A.J. Sedlacek and C.A Wight, J Phys. Chem 93 (1989) 509.
[19] R.P. Wayne, Atmos. Environ. 21 (1987) 1683
[20] J. Fournier, H.H. Mohammed, J. Deson and D. Maillard, Chem. Phys. 70 (1982) 39
[21] Z. Mielke, M Hawkins and L Andrews, J Phys Chem 93 (1989) 558
[22] J N. Crowley and J.R. Sodeau, J Phys Chem. 93 (1989) 3100